Design of Waveguide Head-Up Display with Embedded Gratings

Meng You (尤 勐)[1,2], Zhanhua Huang (黄战华)[1,2*], and Huaiyu Cai (蔡怀宇)[1,2]

[1] *College of Precision Instrument and Optoelectronics Engineering, Tianjin University, Tianjin 300072, China*
[2] *Key Laboratory of Opto-Electronics Information Technology (Tianjin University), Ministry of Education, Tianjin 300072, China*

[*] *Corresponding author: zhanhua@tju.edu.cn*

Received March 5, 2012; accepted May 25, 2012

Abstract The embedded grating is applied in the waveguide head-up display. As an incident and exit coupling grating, it can satisfy the highly efficient and uniform display for large field of view (FOV) based on rigorous coupled wave analysis (RCWA). Compared with holograms in previous designs, it can be easily duplicated with high reliability and low costs. The total internal reflection condition is discussed in the plate, and the revolving problems are discussed in the rod. The system is simulated in software with good optical performance: 50-mm exit pupil, a 30° × 20° FOV, distortion of less than 0.5%, and low aberration. The results are useful for transparent display in vehicles or wearable helmets.

OCIS codes: 000.4430, 050.1970, 220.3620
doi: 10.3788/CJL201239.0916001

1 Introduction

The head-up display (HUD) or helmet-mounted display (HMD), is used to reduce the burden on pilots by showing the scenes outside and instrument information inside at the same time. Traditional HUD or HMD applies the off-axis method to display images that need complex lenses, heavy and occupying too much space[1]. To solve the problem, a waveguide hologram (WGH) is used by folding the optical paths inside to make the structure lighter and more integrated[2,3]. Eisen *et al.*[4] has designed a planar display by placing three holograms in a single transparent substrate. Yan *et al.*[5] provides another approach by embedding reflective-volume holograms in a conical mounting configuration. However, both methods apply volume holograms in the design, which are hard to preserve and difficult for precise duplication[6,7]. They would affect industrial mass production, reduce reliability, and increase costs. And according to Kogelnik's theory[8], the efficiency could change dramatically with wide incident angles, especially for volume holograms, which would vary the uniformity of different FOVs.

Learning from several patents from BAE systems in the United Kingdom[9-11], in this paper, we replace the hologram with embedded gratings in device and designs the WGH-HUD system. Compared with the patents, the structure of WGH-HUD is improved by changing the coupling method between the rod and the plate. Details not revealed in the patents are set and discussed. With the FOV set to 30°×20°, the coupled beam is proven to make the total internal reflection (TIR) in the waveguide, and the parity of diffraction number in the rod is discussed. On the basis of rigorous coupled wave analysis (RCWA), the embedded gratings can serve for incident and exit coupling in devices, with easy duplication and stable efficiency of wide incident angles. Applying the gratings in WGH-HUD, the entire system is simulated in software, with λ changing from 515 to 550 nm. The good optical performance shows that WGH-HUD could be applied in the vehicle or wearable display.

2 Brief Description of WGH-HUD

The structure of WGH-HUD comprises two parts, the rod and the plate (Fig. 1(a)). There are four gratings embedded inside: G1, G2, G3, and G4. The collimated beam from the organic light-emitting diode (OLED) is incident on the rod in the direction of A (Fig. 1(b)).

It would be diffracted by G1 and then make the revolving TIR in the direction of B. In this process the beam would be gradually diffracted out into the plate by G2. The G3 in the plate would diffract the incident beam to make the TIR in the direction of C. When the beam reaches the area of G4, it would be gradually diffracted out to the observing point with a large exit pupil.

In WGH-HUD there are two kinds of gratings, G1 and G3, for incident coupling and two kinds, G2 and G4, for exit coupling. For G1 and G3 the diffraction efficiency should be high and stable with wide incident angels so as to retain the energy from different FOVs of

the OLED. For G2 and G4 the efficiency should increase gradually in the direction of the TIR so as to enlarge the exit pupil and make the energy uniform.

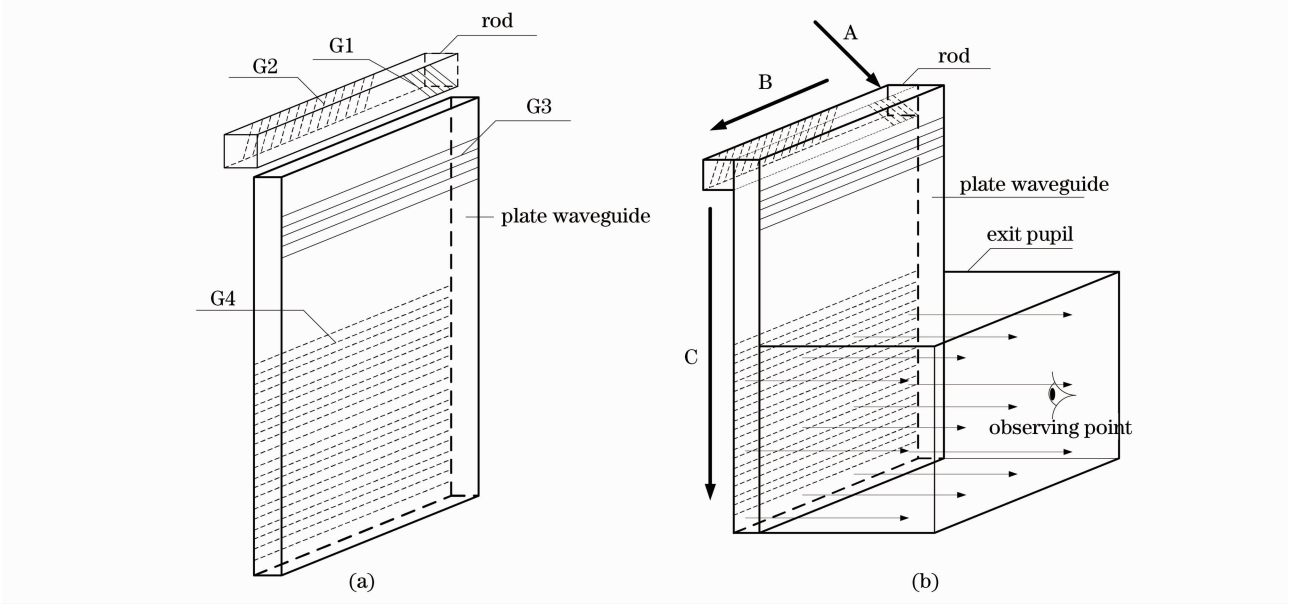

Fig. 1. Structure of WGH-HUD. (a) Divided parts of the rod and the plate and (b) a brief description of the function of WGH-HUD.

3 Detailed Analysis of the Structure

3.1 TIR Conditions with Large Fields of View

The wavelength of the OLED is often set from 515 to 550 nm, with a central λ of 532 nm. With the collimation of the projection lens, the FOV is generally set as $30^\circ \times 20^\circ$, with 30° for the horizontal angle a in the xz-plane and 20° for the vertical angle b in the xy-plane (Fig. 2(a)). After coupling into the waveguide, the diffraction angles with the bottom should be less than 45° to satisfy the TIR condition. With the material set as poly (methyl methacrylate) (PMMA), the cycle T is set as 410 nm.

With a and b changing in the range of $30^\circ \times 20^\circ$, the diffraction angle with the bottom is shown in Fig. 2(b). The results show that when angle a is from -15° to 15° and angle b is from -5° to 15°, the angle with the bottom is in $[20^\circ, 45^\circ]$, satisfying the TIR condition and guaranteeing enough diffraction numbers in the waveguide.

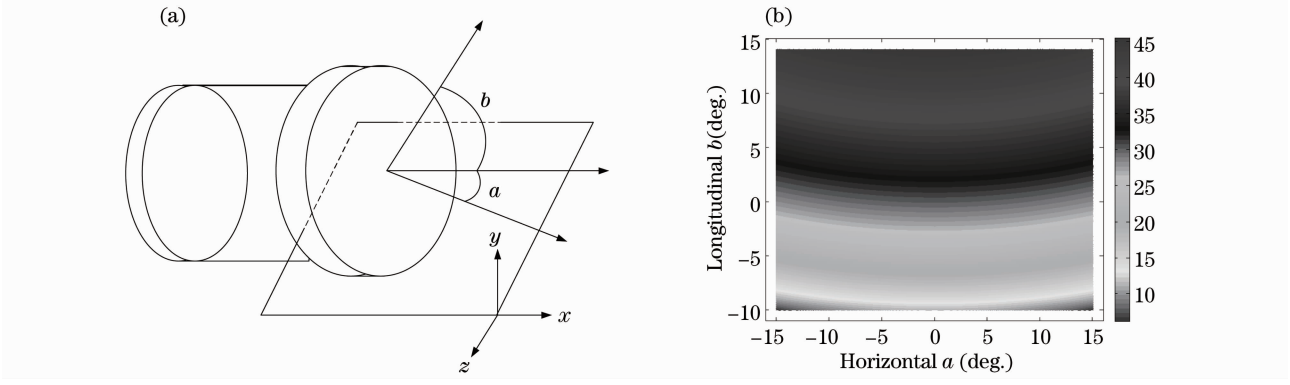

Fig. 2. (a) FOV from the collimated OLED and (b) diffraction angles with the bottom.

3.2 Revolving TIR in the Rod

The beam would make the revolving TIR in the rod save space and volume, with fringes of G1 and G2 set to 45° (Fig. 3). Taking the perpendicular incidence as an example, the diffracted beam from G1 would make rotated propagation in the rod and exit when it reaches G2. Before the exit there are two kinds of situations, even and odd times of reflection.

When the incident angle is in the range of $30^\circ \times 20^\circ$, most of the beams would be diffracted to the bottom, with even times of reflection, because of the 45° fringe of G1 and the cross-sectional size of the rod. If the

beam is diffracted to the opposite side, which means the time is odd, the incident plane would rotate 90° from the original (Fig. 3(c)).

According to the improved grating function $Gm\lambda = \cos\varepsilon(\sin\alpha + \sin\beta)$[12], when the rotated angle $\varepsilon = 90°$, there would be no high diffraction orders except zero[13].

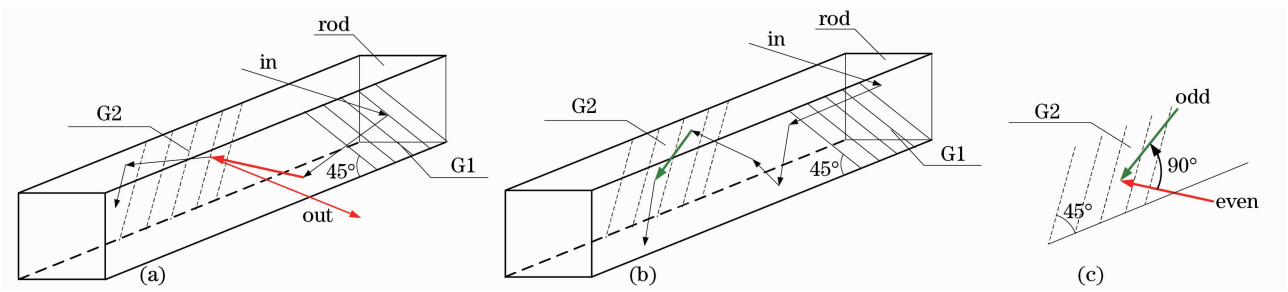

Fig. 3. (a) Even times, (b) odd times, and (c) 90° rotation from the original incident plane.

4 Calculation of Embedded Gratings

4.1 Structure of the Grating

As mentioned in Section 2 there are two kinds of gratings in WGH-HUD for incident and exit coupling, respectively (Fig. 4). The cycle is set as T, the groove depth is d, and the thickness of the film is x. The lower substrate in Fig. 4(a) and the substrate in Fig. 4(b) are made of PMMA, while the higher substrate in Fig. 4(a) is made of silver (Ag). The film in both structures is made of titanium dioxide (TiO_2)[14]. With ion-beam etching and e-beam evaporation[15,16], these gratings could be precisely duplicated in mass production, increasing reliability and reducing costs.

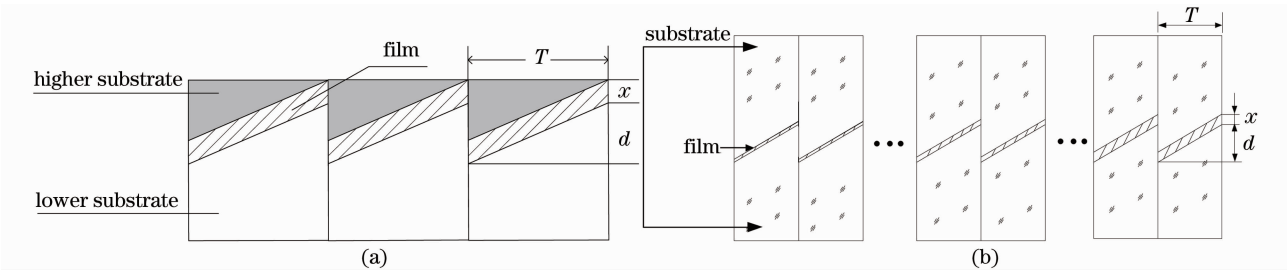

Fig. 4. (a) Incident coupling grating and (b) exit coupling grating.

4.2 Efficiency Analysis

The cycle T is 410 nm, and the groove depth d is 220 nm. With transverse electric (TE)-polarized perpendicular incidence, the relation curve is calculated between the first-order diffraction efficiency (1st DE) and the film thickness x based on RCWA[17-19].

Figure 5(a) shows the results of incident coupling gratings, such as G1 and G3. When x changes from 50 to 150 nm, the 1st DE is about 90%, while other orders are below 5%, which means the coupling efficiency is close to 90% with little loss.

In WGH-HUD the exit pupil is stretched in two dimensions by exit coupling gratings, such as G2 and G4, which requires increasing efficiency to achieve uniform display. If the diffraction number of times in the waveguide is n, the efficiency should make corresponding increments:

$$\eta_1 = \frac{1}{n}, \eta_2 = \frac{1}{n-1}, \cdots\cdots \eta_{n-2} = \frac{1}{3},$$

$$\eta_{n-1} = \frac{1}{2}, \eta_n = 1, (n = 1, 2, \cdots).$$

The efficiencies are all below 33% except η_n and η_{n-1}. As the efficiency should be low enough to ensure the transmission of scenes outside, η_n and η_{n-1} are abandoned. The total efficiency would be larger than 80% with $n = 10$ and 90% with $n = 20$.

Figure 5(b) shows the results of exit coupling gratings, such as G2 and G4. When the film thickness x changes from 0 to 60 nm, the 1st DE increases gradually with a peak of 37%, with other nonzero orders approaching zero. The peak efficiency is larger than 33%, which could satisfy the increasing efficiency in WGH-HUD by varying x at different locations on the waveguide. And the suppression of the nonzero orders could reduce the energy loss and scattered imaging beams.

With FOV of 30° × 20°, the efficiency barely changes with the incident angle (Fig. 5), which is conductive to the highly efficient and uniform display in the entire FOV.

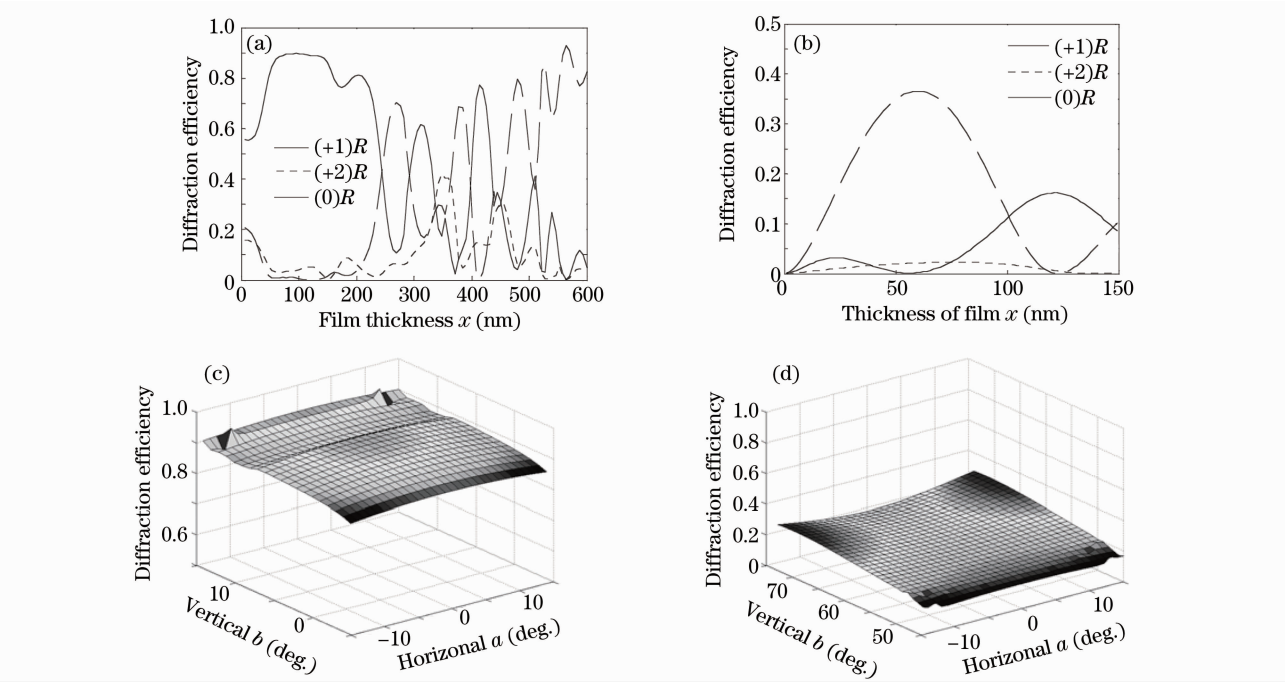

Fig. 5. (a) Incident coupling grating, (b) exit coupling grating, (c) efficiency surface with $x = 96$ nm, and (d) efficiency surface with $x = 30$ nm.

5 Simulations

The optical system of WGH-HUD is simulated by CODE V® (software from ORA®) (Fig. 6). The organic light-emitting diode (OLED) (20 mm in diagonal) is chosen as the image source with 1024 × 768 pixels. The wavelength varies from 515 to 550 nm, with a central λ of 532 nm. The collimated group comprises seven glass lenses with an effective focal length of 37.5 mm. It has a 10-mm stop aperture and a 30° × 20° FOV. For the entire system the exit pupil is 50 mm in diameter, with an exit pupil distance (EPD) of 150 mm (Fig. 6(a)) and 20 mm (Fig. 6(b)) applied in vehicles or wearable helmets.

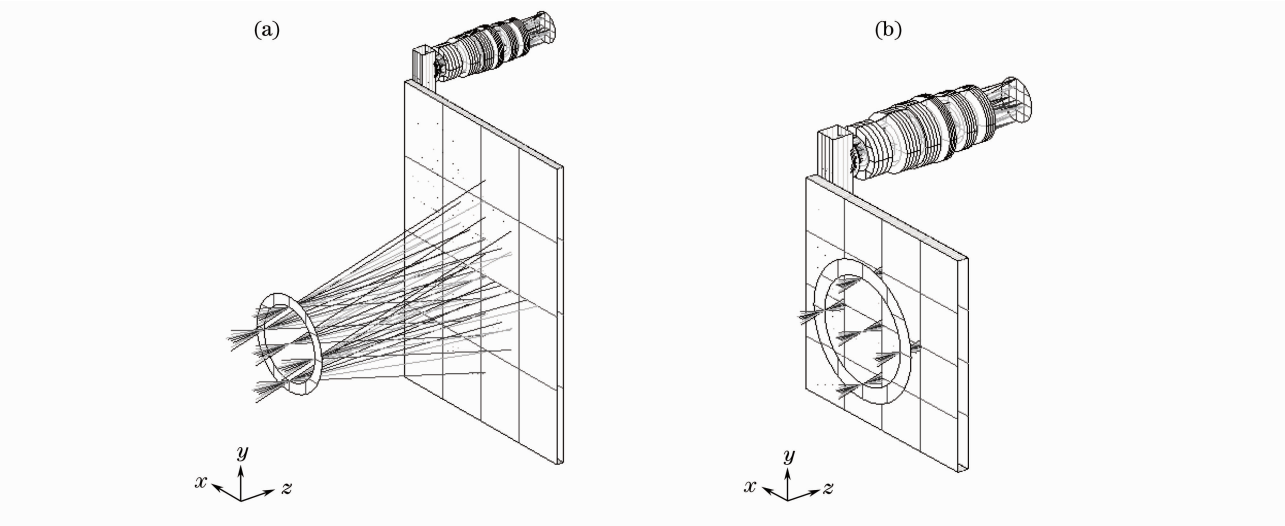

Fig. 6. (a) 150-mm EPD and (b) 20-nm EPD.

The G1≈G4 in WGH-HUD is simulated by setting the linear grating on the surface with different values in the grating directions x and y. The rays are traced with nonsequential surfaces in the waveguide, which is 5-mm thick for the plate and 10 × 10 (mm) for the cross section of the rod.

After optimization, Fig. 7(a) shows the spot diagram with a root mean square (RMS) diameter, which is less than 4.1 μm. Ray aberration is plotted in Fig. 7(b), which is less than 0.01 for the entire FOV.

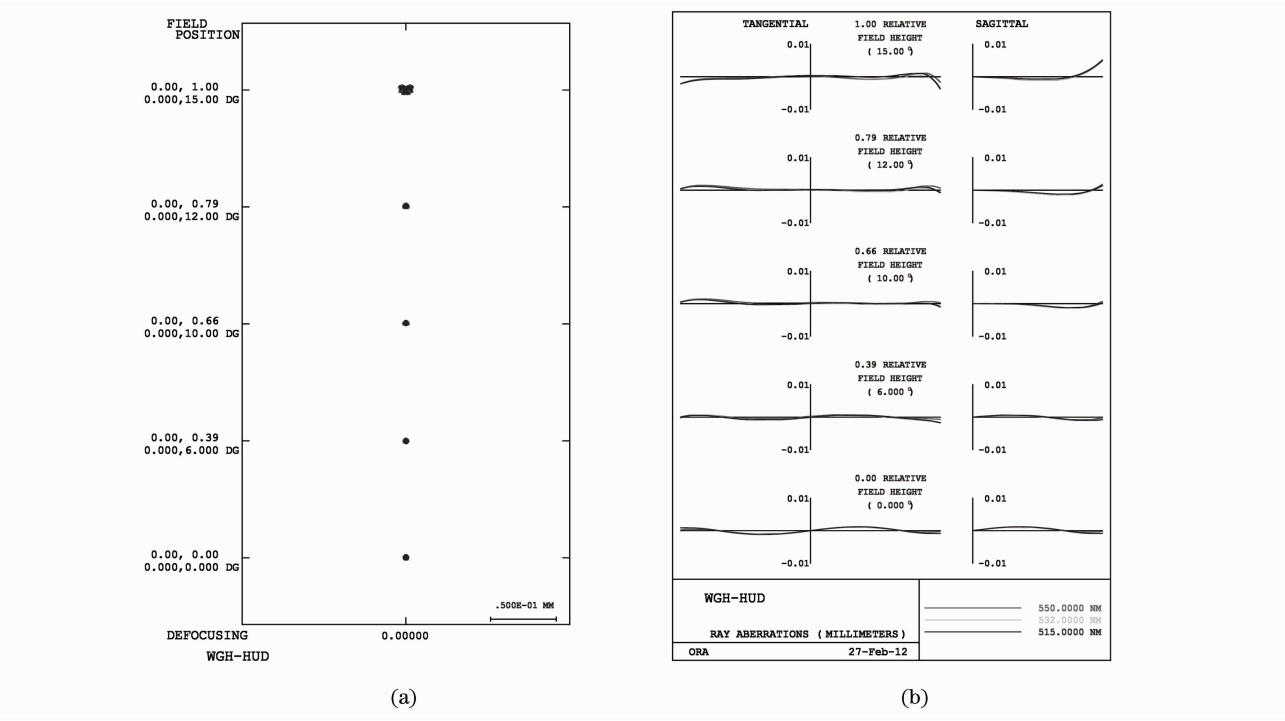

(a) (b)

Fig. 7. (a) Spot diagram with rms diameter less than 4.1 μm and (b) ray aberration less than 0.01.

Figure 8(a) shows the modulation transfer function (MTF) curve of the simulated system, with an average value of 85% at 40 line cycles/mm, close to the diffraction limit. The astigmatic field curve and the distortion are less than 0.5% for the entire FOV.

The results have shown good optical performance of the simulated WGH-HUD system, with high resolution, little ray aberration, and little distortion. And the even number of gratings embedded does not contribute to the chromatic aberration. A large FOV and exit pupil are achieved with different EPDs to be applied in vehicles or wearable helmets.

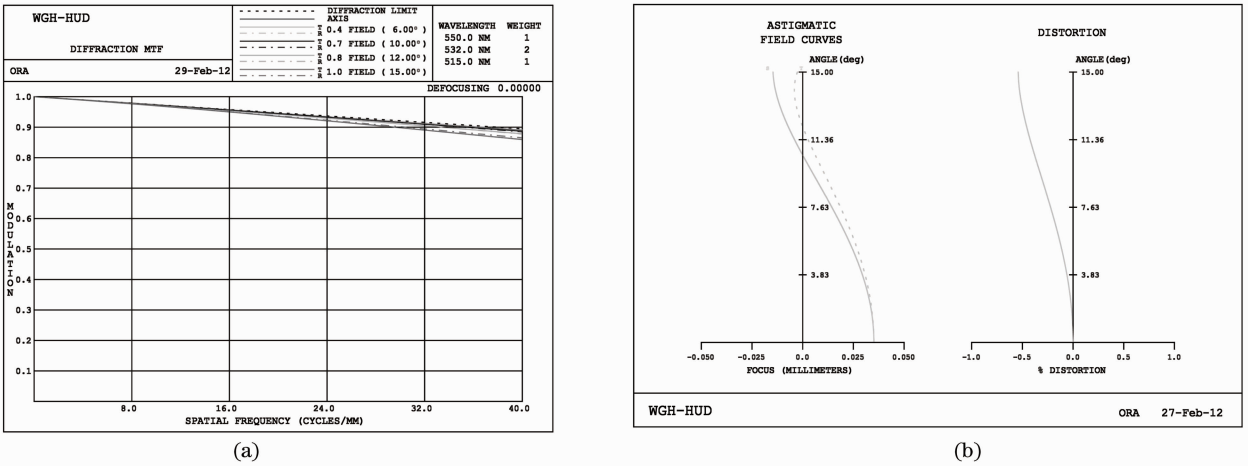

(a) (b)

Fig. 8. (a) MTF and (b) astigmatic field curves and the distortion.

6 Conclusions

The embedded grating is used in the design of WGH-HUD for incident and exit coupling. On the basis of calculations of RCWA, it can satisfy the highly efficient and uniform display for large FOVs. Compared with holograms it can be easily and precisely duplicated with high reliability and low costs. Considering TIR conditions in rods and plates, WGH-HUD with novel gratings is simulated in software with a large FOV and exit pupil. The results could be useful for practical applications of transparent display in vehicles or wearable helmets.

References

1 O. Cakmakci. Head-worn displays: a review [J]. *J. Dis. Tech.*, 2006, **2**(3): 199～216

2 Y. Amitai, S. Reinhom, and A. A. Friesem. Visor-display design based on planar holographic optics [J]. *Appl. Opt.*, 1995, **34**(8): 1352～1356

3 Y. Amitai, A. A. Friesem, and V. Weiss. Holographic elements with high efficiency and low aberrations for helmet displays [J]. *Appl. Opt.*, 1989, **28**(15): 3405～3416

4 L. Eisen, M. Meyklyar, M. Golub *et al.*. Planar configuration for image projection [J]. *Appl. Opt.*, 2006, **45**(17): 4005～4011

5 Z. J. Yan, W. Li, Y. Zhou *et al.*. Virtual display design using waveguide hologram in conical mounting configuration [J]. *Opt. Eng.*, 2011, **50**(9): 094001-1～094001-8

6 H. X. Zhou and Y. F. Cheng. Design, Manufacturing and Application of Holographic Optics (in Chinese) [M]. Beijing: Chemical Industry Press, 2006

7 R. J. Collier, C. B. Burdkhardt, and L. H. Lin. Optical holography [M]. San Diego: Academic Press, 1971

8 H. Kogelnik. Coupled wave theory for thick hologram gratings [J]. *Bell. Sys. Tech. J.*, 1967, **48**(9): 2909～2946

9 A. Cameron. The application of holographic optical waveguide technology to *Q*-Sight™ family of helmet mounted displays [C]. *SPIE*, 2009, **7326**: 73260H-1～73260H-11

10 S. Michael, and V. Mohmed, "A projection display with a rod-like, rectangular cross-section waveguide and a plate-like waveguide, each of them having a diffraction grating", W. O. Patent 2007/029034 (March 15, 2007)

11 S. Michael, D. Valera, and M. Salim. "Improvements in optical waveguides", W. O. Patent 2010/122329 (October 28, 2010)

12 C. Palmer. Diffraction Grating Handbook (6th) [M]. New York: Newport Corporation, 2005

13 D. Zhang, L. Yuan, J. Chen *et al.*. Design of guided mode resonant filters for authentication applications through azimuthal angles varying [J]. *Chin. Opt. Lett.*, 2008, **6**(10): 776～778

14 G. Ghosh. Handbook of Thermo-Optic Coefficients of Optical Materials with Applications (Academic Press, San Diego, 1998)

15 N. Wang, C. Y. Wei, J. D. Shao *et al.*. Experimentation of deposition rate control of SiO_2 by e-beam auto-sweeping [J]. *Chinese J. Lasers*, 2010, **37**(10): 2615～2619

16 Z. W. Xu, F. Z. Fang, S. Q. Zhang *et al.*. Fabrication of complicated micronano structures using focused ion beam milling method [J]. *J. Tianjin Univ.*, 2009, **2**(1): 91～94

17 T. Sun, Y. Jin, J. Shao *et al.*. Guided-mode resonances in multimode planar periodic waveguides [J]. *Chin. Opt. Lett.*, 2010, **8**(6): 557～559

18 Z. Wang, Y. Wu, Z. Xia *et al.*. Multimode resonance bandpass filter with twin wideband channels [J]. *Chin. Opt. Lett.*, 2011, **9**(8): 080501-1～080501-3

19 M. G. Moharam. Stable implementation of the rigorous coupled wave analysis for surface-relief gratings enhanced transmittance matrix approach [J]. *J. Opt. Soc. Am. A*, 1995, **12**(5): 1077～1086